RNF186/EPHB2 Axis Is Essential in Regulating TNF Signaling for Colorectal Tumorigenesis in Colorectal Epithelial Cells

Huazhi Zhang,*[,1] Zhihui Cui,*[,1] Ting Pan,[†,‡,1] Huijun Hu,*[,1] Ruirui He,[†,‡] Ming Yi,[†,‡] Wanwei Sun,* Ru Gao,* Heping Wang,* Xiaojian Ma,* Qianwen Peng,* Xiong Feng,* Shuyan Liang,[§] Yanyun Du,[†,‡] and Chenhui Wang[†,‡]

The receptor tyrosine kinase EPHB2 (EPH receptor B2) is highly expressed in many human cancer types, especially in gastrointestinal cancers, such as colorectal cancer. Several coding mutations of the *EPHB2* gene have been identified in many cancer types, suggesting that EPHB2 plays a critical role in carcinogenesis. However, the exact functional mechanism of EPHB2 in carcinogenesis remains unknown. In this study, we find that EPHB2 is required for TNF-induced signaling activation and proinflammatory cytokine production in colorectal epithelial cells. Mechanistically, after TNF stimulation, EPHB2 is ubiquitinated by its E3 ligase RNF186. Then, ubiquitinated EPHB2 recruits and further phosphorylates TAB2 at nine tyrosine sites, which is a critical step for the binding between TAB2 and TAK1. Due to defects in TNF signaling in RNF186-knockout colorectal epithelial cells, the phenotype of colitis-propelled colorectal cancer model in RNF186-knockout mice is significantly reduced compared with that in wild-type control mice. Moreover, we find that a genetic mutation in EPHB2 identified in a family with colorectal cancer is a gain-of-function mutation that promoted TNF signaling activation compared with wild-type EPHB2. We provide evidence that the EPHB2-RNF186-TAB2-TAK1 signaling cascade plays an essential role in TNF-mediated signal transduction in colorectal epithelial cells and the carcinogenesis of colorectal cancer, which may provide potential targets for the treatment of colorectal cancer. ***The Journal of Immunology*****, 2022, 209: 1796–1805.**

The EPH receptor B2 (EPHB2) belongs to the EPH receptor family, which is the largest tyrosine kinase receptor family in humans. EPH receptor family proteins can be further divided into EPH receptor A and EPH receptor B classes according to sequence identity (1, 2). The EPH receptor signaling axis is involved in a wide range of biological processes, including cell migration, axon guidance, formation of tissue boundaries, colorectal stem cell localization, synapse formation, and angiogenesis (3–9). This activity is achieved through the binding of EPH receptors to their ligand ephrins. The binding of EPH receptors and ephrins leads to bidirectional signaling and results in cell–cell repulsion (9). In addition to the important role of EPH receptors in development, accumulating evidence suggests their potential role in tumorigenesis, and EPHB2 is especially closely related to the proliferation, metastasis, and angiogenesis of many types of cancers (1, 2, 4, 10–12). For example, altered EPHB2 expression levels are observed in colorectal cancer, gastric cancer, lung carcinoma, melanoma, and neuroblastomas, among others, and prognosis is also closely correlated with EPHB2 expression levels (13, 14). The fact that several mutations within the EPHB2 coding region have been identified in prostate cancer and colorectal cancer further confirms its potential role in cancers (15, 16), whereas the functional mechanism of EPHB2 in the regulation of carcinogenesis in different cancers remains unclear.

TNF is mainly a type II transmembrane protein that acts as a homotrimer, and membrane-integrated TNF is cleaved by the metalloprotease TNF-α converting enzyme (TACE) to produce soluble TNF-α (17). TNF has a variety of biological functions, and its major function is to induce the proinflammatory response through its receptors TNFRI and TNFRII (18). The engagement of TNF and TNFR causes trimerization of the receptor and recruitment of TRADD (TNFR-associated death domain), TRAF2 (TNFR-associated factor 2), FADD (Fas-associated death domain), and RIP (receptor-interacting protein), and ubiquitination of RIP further

*Key Laboratory of Molecular Biophysics of the Ministry of Education, National Engineering Research Center for Nanomedicine, College of Life Science and Technology, Huazhong University of Science and Technology, Wuhan, China; [†]The Key Laboratory for Human Disease Gene Study of Sichuan Province and the Department of Laboratory Medicine, Sichuan Provincial People's Hospital, University of Electronic Science and Technology of China, Chengdu, China; [‡]Research Unit for Blindness Prevention of the Chinese Academy of Medical Sciences (2019RU026), Sichuan Academy of Medical Sciences and Sichuan Provincial People's Hospital, Chengdu, Sichuan, China; and [§]Wuhan Biobank Co., Ltd., Wuhan, China

[1]H.Z., Z.C., T.P., and H.H. contributed equally to this work.

ORCIDs: 0000-0001-7689-5638 (H.H.), 0000-0002-8357-0222 (H.W.).

Received for publication March 28, 2022. Accepted for publication August 8, 2022.

This work was supported by the Original Exploration Program of Foundation for Innovative Research Groups of the National Natural Science Foundation of China Grant 82150102 (to C.W.), the National Science Fund for Distinguished Young Scholars (82225029, to C.W.), National Key Research and Development Program of China Grant 2020YFA0710700 (to C.W.), Key Research and Development Program of Sichuan Province Grant 22ZDYF3738 (to C.W.), National Natural Science Foundation of China Grant 82101859 (to W.S.) and by the Postdoctoral Foundation of Sichuan Provincial People's Hospital (2022BH01, to R.R.H. and 2022BH07, to M.Y.).

H.Z., Z.C., T.P. and H.H. performed the experiments with the assistance from R.H., M.Y., W.S., Y.D., R.G., H.W., X.M., Q.P., Z.C., X.F., and S.L.; H.Z. and C.W. analyzed the data; and C.W. wrote the manuscript and supervised the project with Y.D.

The RNA-seq data presented in this article have been submitted to Gene Expression Omnibus under accession number GSE197895.

Address correspondence and reprint requests to Dr. Yanyun Du and Prof. Chenhui Wang, Sichuan Provincial People's Hospital, University of Electronic Science and Technology of China, Section 2 of Jianshe North Road, Chenghua District, Chengdu City, China 610054. E-mail addresses: yanyundu1@163.com and wangch@uestc.edu.cn

The online version of this article contains supplemental material.

Abbreviations used in this article: AOM, azoxymethane; coIP, coimmunoprecipitation; DSS, dextran sodium sulfate; EPHB2, EPH receptor B2; gRNA, guide RNA; HA, hemagglutinin; KD, kinase-dead; KO, knockout; RNA-seq, RNA sequencing; RT, reverse transcription.

recruits the TAK1/TAB2/TAB3 complex for the activation of the downstream IKK complex and NF-κB/MAPK signaling pathway (17–20). TNF is closely related to the carcinogenesis of colorectal cancers (21, 22). For example, TNF activates stromal COX-2 signaling for the proliferation and invasiveness of colon cancer epithelial cells (23). TNF and IL-17A synergistically activate glycolysis and growth factor production in colitis-propelled colorectal cancer cells (24). TNF and IL-6 synergistically activate NF-κB and STAT3 to promote colorectal cancer cell proliferation (25). Administration of etanercept, a specific antagonist of TNF, has a therapeutic effect on dextran sodium sulfate (DSS) + azoxymethane (AOM)–induced mouse colitis-propelled colon cancer (26). A clinical study found that serum TNF levels are significantly increased in colorectal cancer patients compared with healthy individuals (27). Overall, these findings indicate that TNF plays an essential role in the tumorigenesis of colorectal cancer, whereas the TNF-driven events in colorectal epithelial cells remain elusive.

In this study, we find that in colorectal epithelial cells, TNF induces RNF186-mediated EPHB2 ubiquitination, and ubiquitinated EPHB2 recruits TAB2 for phosphorylation at nine different tyrosines, which is required for the binding of TAK1 and downstream signaling activation. In RNF186-knockout (KO) mice, although DSS-induced colitis is more severe than that in wild-type control mice, RNF186-KO mice exhibited marked reductions in the number and size of tumors induced by DSS+AOM. Moreover, we provide evidence that a genetic mutant of EPHB2 (D862N) identified in a colorectal cancer family is a gain of function in the TNF signaling pathway. This study not only explores the mechanistic role of EPHB2 in TNF signaling in colorectal epithelial cells but also provides a potential target for the treatment of human colorectal cancer.

Materials and Methods

Mice

The *RNF186*$^{-/-}$ mice were made by Cyagen Biosciences by the CRISPR-Cas9 technique as demonstrated in the previous study (28). The guide RNA (gRNA) sequences to deplete *RNF186* are as follows: gRNA1, 5′-TCATTGCCTTGGGGCCCACCGGG-3′; gRNA2, 5′-CCCCTGTCCGCTGTGCCGAAAGG-3′. The 188-bp DNA fragment was depleted by these two gRNAs, which was confirmed by genotyping. The depletion of the 188-bp DNA fragment resulted in a frameshift for the rest of the *RNF186* cDNA. To avoid possible off-target editing of the genome, the mice were breed for six generations with mice of the C57BL/6 background before performing any experiments. Experimental protocols were approved by the Institutional Animal Care and Use Committee of the Tongji Medical College, Huazhong University of Science and Technology.

Cells

293T (AtaGenix, ata-c11001) and Ls174t cells (American Type Culture Collection, CL-188) were maintained in DMEM (M&C Gene Technology, CM10013) plus 10% FBS and 1% penicillin-streptomycin.

Reagents

The following Abs were used: anti–p-IκBα Ab (Cell Signaling Technology, 2859), anti–p-JNK Ab (Cell Signaling Technology, 4668), anti–p-ERK Ab (Cell Signaling Technology, 4370), anti–p-p38 Ab (Cell Signaling Technology, 4511), anti-MAP1LC3B (Cell Signaling Technology, 2775), anti–p-STAT3 Ab (Cell Signaling Technology, 9145), anti-FLAG (Cell Signaling Technology, 14793), and anti-hemagglutinin (HA) (Cell Signaling Technology, 3724) for Western blotting. The Abs of anti-FLAG (F1804) and anti-HA (H9658) for immunoprecipitation were purchased from Sigma-Aldrich. Anti–P-Y (sc-508), anti-EPHB2 (sc-130068), anti-HSP90 (sc-13119), anti-ACTB (sc-70319), anti-His (sc-8036), and anti-Ub (sc-8017) Abs were purchased from Santa Cruz Biotechnology. The Ab of anti-MYC was purchased from GNI (GNI4110-MC). Anti–p-EPHB2 Ab was purchased from Thermo Fisher Scientific (PA5-40236). DSS (molecular mass, 40,000 Da) was purchased from MP Biomedicals (160110). AOM was purchased from Sigma-Aldrich (A5486). R7050 was purchased from MCE (HY-110203).

Immunoblot and immunoprecipitation

Cells were harvested and lysed on ice in a lysis buffer containing 0.5% Triton X-100 (Solarbio Life Sciences, T8200), 20 mM HEPES (pH 7.4), 150 mM NaCl, 12.5 mM β-glycerophosphate (ApexBio, 13408-09-8), 1.5 mM $MgCl_2$, 10 mM NaF, 2 mM DTT, 1 mM sodium orthovanadate, 2 mM EGTA, 20 mM aprotinin (TargetMol, C0001), and 1 mM PMSF (MCE, 329-98-6) for 30 min on ice, followed by centrifugation at 13,680 × *g* for 15 min to extract clear lysates. For immunoprecipitation, cell lysates were incubated with 1 μg of Ab at 4°C overnight, followed by incubation with protein A Sepharose or protein G Sepharose beads (Solarbio, P2040) for 4 h at 4°C, and the beads were washed four times with lysis buffer and the precipitates were eluted with 2× sample buffer. Elutes and whole-cell extracts were resolved on SDS-PAGE followed by immunoblotting with Abs. Densitometric quantification of Western blot was performed on images of scanned films using ImageJ, and the band detection was within the linear range.

Mass spectrometry identification

293T cells were cotransfected with HA-EPHB2 and Myc-TAB2, followed by immunoprecipitation with anti-Myc Abs. Proteins were eluted and analyzed by mass spectrometry for identification of the tyrosine sites.

Samples were reduced and alkylated in DTT and iodoacetamide followed by trypsin digestion overnight. Digested samples were injected onto an Agilent Zorbax 300SB-C18 0.075- × 150-mm column on an Eskigent NanoLC system coupled with a Thermo LTQ-ETD-Orbitrap. Advion TriVersa NanoMate served as the nano-ion spray source. Tandem mass spectrometry data were searched against the RefSeq human protein database by Sorcerer SEQUEST. The searched dataset was processed by Trans-Proteomics Pipeline and filtered with PeptideProphet.

In vivo ubiquitination experiment

Cells were harvested by washing with cold PBS and then were lysed with a 1% SDS solution. The lysates were then sonicated for 15 s on ice to disrupt the DNA. The lysates were boiled at 95°C for 5 min to dissociate the protein interaction. The boiled samples were diluted with coimmunoprecipitation (coIP) buffer to 0.1% SDS and incubated on ice for 30 min, followed by centrifugation at 13,680 × *g* for 5 min, after which the pellet was discarded. The supernatants were then incubated with protein A/G Sepharose and Abs against FLAG, and they were rotated at 4°C overnight. The protein A/G Sepharose beads were then pelleted and washed four times with coIP buffer. The precipitates were resolved by SDS-PAGE and subjected to Western blotting with Abs against FLAG or Myc.

Tyrosine phosphorylation detection

For tyrosine phosphorylation experiments, cells were transfected as indicated, followed by lysing with a 1% SDS solution. The lysates were then sonicated for 15 s on ice to disrupt the DNA. The lysates were boiled at 95°C for 10 min to dissociate the protein interaction. The boiled samples were diluted with coIP buffer to 0.1% SDS and then centrifuged at 12,000 rpm for 10 min, after which the pellet was discarded. Cell lysates were incubated with 1 μg of Ab at 4°C overnight, followed by incubation with protein A Sepharose or protein G Sepharose beads for 2 h, and the beads were washed four times with lysis buffer and the precipitates were eluted with 5× sample buffer. The precipitates were resolved by SDS-PAGE and subjected to Western blotting analysis by using anti–p-tyrosine Ab.

Lentivirus-medicated gene KO

pLV-U6g-EPCG and LentiCRISPR-V2 vectors were used for CRISPR-Cas9–mediated gene knockout in cell lines. Briefly, lentivirus vector expressing gRNA was transfected together with package vectors into 293T cells. Forty-eight and 72 h after transfection, virus supernatants were harvested and filtrated with a 0.2-μm filter. Target cells were infected twice and were sorted by flow cytometry–mediated cell sorting or puromycin selection. For some experiments, a single cell was plated into a 96-well plate for a single clone. Isolated single clones were verified by gene KO by Western blot or DNA sequencing. In some case, a pool of GFP-sorted or puromycin-selected cells was used in the experiments.

Quantitative reverse transcription PCR

Total RNA was extracted from the spinal cord with TRIzol (Invitrogen) according to the manufacturer's instructions. On microgram of total RNA for each sample was reverse transcribed using the HiScript II Q RT SuperMix (Vazyme, R223-01). The resulting cDNA was analyzed by quantitative reverse transcription (RT)-PCR using SYBR Green quantitative RT-PCR master mix (Vazyme, Q311-02). All gene expression results are expressed as arbitrary units relative to *Actb* and *GAPDH* (glyceraldehyde-3-phosphate dehydrogenase) expression.

RNA sequencing

For the RNA sequencing (RNA-seq) experiment, Ls174t cells overexpressed with empty vector or hRFN186 were harvested by TRIzol. Samples were sent to BGI for RNA-seq analysis. For the data analysis, gene expression from human RNF186–expressed cells/gene expression from empty vector–expressed cells was calculated as the fold change (the gene expression from empty vector–expressed cells was normalized as 1).

DSS+AOM-induced mice colon cancer

Experiment colorectal tumors was induced with a single AOM injection and three repeated DSS administrations. Eight- to 10-wk old mice ($Rnf186^{+/-}$ and $Rnf186^{-/-}$ littermates on a C57BL/6 background) were injected i.p. with AOM (Sigma-Aldrich) dissolved in PBS at a dose of 10 mg/kg body weight. After 5 d of injection, mice were treated with 2% (w/v) DSS (molecular mass 36,000–50,000 Da; MP Biomedicals, 160,110) in drinking water ad libitum for 5 d, then followed by regular water for 16 d. This process of DSS was repeated twice for a total of three cycles. The body weight was assessed at least 4 d per week throughout the course of the experiment. Mice were sacrificed 8 wk after the last DSS cycle. Colons were removed and cut longitudinally and then flushed with PBS carefully to remove feces. All of the colon tumors were grossly counted and each tumor was measured for the largest dimension with sliding calipers in a blinded fashion. All tumors of every mice were then categorized based on size (<2 mm, 2–4 mm, or >4 mm). Part of the representative tumors was fixed in 4% paraformaldehyde and embedded in paraffin for histology analysis. Another part of the tumors was prepared for subsequent molecular biological investigations.

Statistical analysis

Statistical significance between two groups was determined by an unpaired two-tailed *t* test, multiple-group comparisons were performed using one-Way ANOVA, and the weight change curve was analyzed by a two-way ANOVA test for multiple comparisons. A p value <0.05 was considered to be significant. Results are shown as means, and the error bar represents the SEM as indicated in the figure legends. All of the statistical analyses were done by using GraphPad Prism 6.01 software.

Data availability

The datasets generated during and/or analyzed during the current study are available from the corresponding author on reasonable request. The RNA-seq data have been deposited into the Gene Expression Omnibus database under the accession number GSE197895 (https://www.ncbi.nlm.nih.gov/geo/query/acc.cgi?acc=GSE197895).

Results

EPHB2 is critical for TNF signaling activation in colorectal epithelial cells

In a previous study, we showed that RNF186 functions by mediating K27-linked ubiquitination of EPHB2 at lysine K892, which is critical for ephrin-B1/EPHB2 axis–induced autophagy in colorectal epithelial

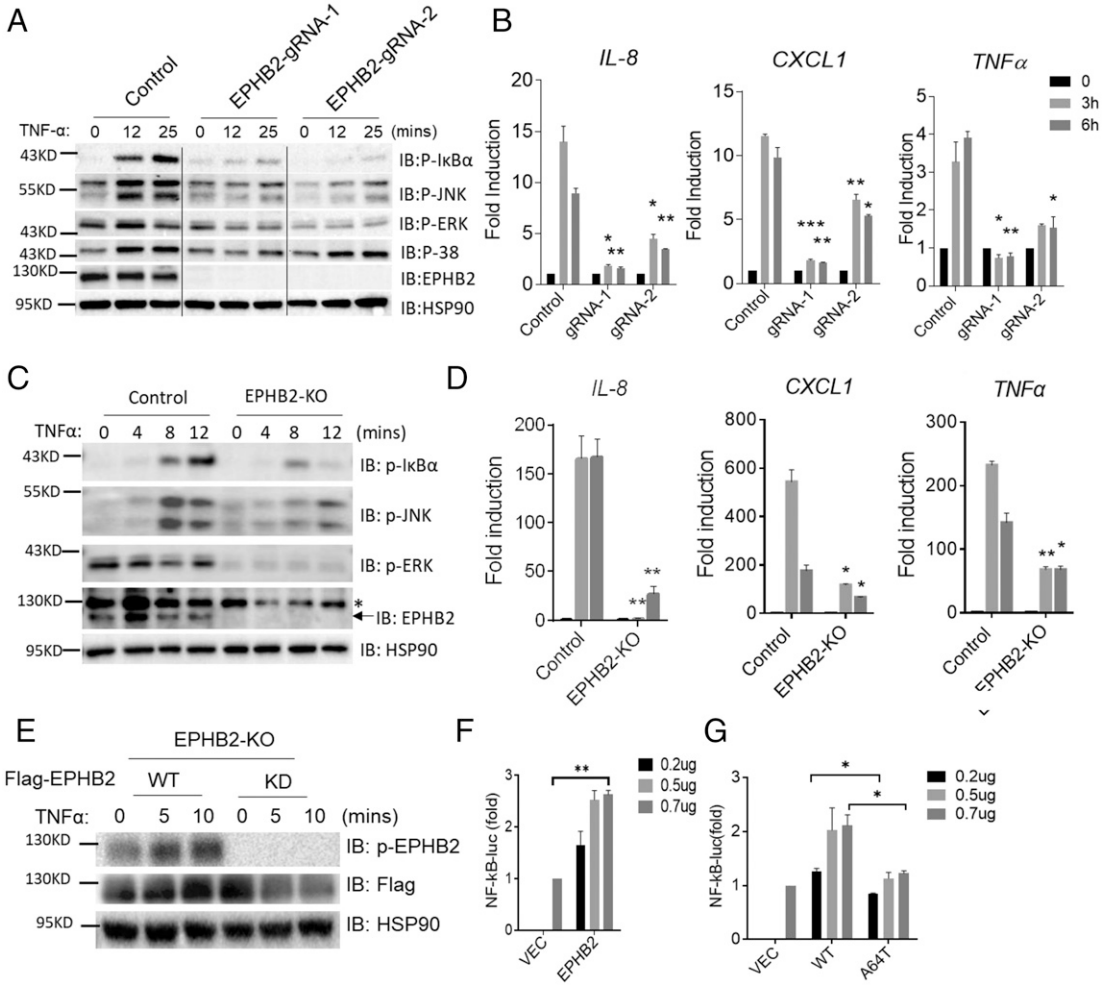

FIGURE 1. EPHB2 is required for TNF-induced signaling activation in colorectal epithelial cells. (**A** and **B**) Control Ls174t cells or EPHB2-KO Ls174t cells were treated with TNF (100 ng/ml) for the indicated time, followed by Western blot or RT and real-time PCR analysis of indicated proteins (A) or mRNA (B) expression. PD, EPHB2 phosphorylation site mutant. (**C** and **D**) Control 293T cells or EPHB2-KO 293T cells were treated with TNF (50 ng/ml) for the indicated time, followed by Western blot or RT and real-time PCR analysis of indicated proteins (C) or mRNA (D) expression. (**E**) EPHB2-KO 293T cells were transfected with wild-type EPHB2 or EPHB2 KD mutant for 24 h, and cells were stimulated with TNF (50 ng/ml) for the indicated time, followed by Western blot analysis of indicated proteins. (**F** and **G**) 293T cells were transfected with indicated plasmids for 24 h, followed by reporter assay analysis of NF-κB activity. *$p < 0.05$, **$p < 0.01$, ***$p < 0.001$ based on two-sided unpaired *t* test for (B), (D), (F), and (G). All error bars represent SEM of technical replicates. Data are representative of three independent experiments.

cells (28). Therefore, we explored whether EPHB2 was also involved in TNF signaling activation in colorectal epithelial cells. Consistent with the role of RNF186 in the TNF signaling pathway, we found that EPHB2-KO Ls174t cells also showed defects in TNF signaling activation and gene expression (Fig. 1A, 1B). This phenomenon was also observed in 293T cells. Specifically, EPHB2 deficiency resulted in significant attenuation of signal transduction and proinflammatory gene expression (Fig. 1C, 1D). Meanwhile, we examined the levels of TNFR1 in EPHB2–wild-type and EPHB2-KO cells, and we did not find any expressional level changes of TNFR1 in EPHB2-KO cells compared with wild-type cells (Supplemental Fig. 1A, 1B). Next, we found that EPHB2 was activated after TNF stimulation, and these data further confirmed the involvement of EPHB2 in the TNF signaling pathway (Fig. 1E). Overexpression of wild-type EPHB2 significantly activated NF-κB activity in 293T cells (Fig. 1F). The RNF186 A64T variant was associated with susceptibility to ulcerative colitis, and we found that the RNF186 A64T variant exhibited impaired E3 ligase activity for EPHB2 (28, 29). Interestingly, overexpression of the wild-type but not the A64T variant of RNF186 increased NF-κB activity in 293T cells, and these data suggest that ubiquitination of EPHB2 may also be important in TNF-induced signaling (Fig. 1G).

RNF186 is required for TNF signaling activation in colorectal epithelial cells

RNF186 is an ulcerative colitis–susceptible gene. In a previous study, we elucidated its role in intestinal homeostasis by regulating ephrin-B/EPHB2–induced autophagy in colorectal epithelial cells (28). Given that the TNF signaling pathway plays a critical role in colorectal diseases, such as inflammatory bowel disease and colorectal cancers (26), we explored whether RNF186/EPHB2 plays any role in the TNF signaling pathway in colorectal epithelial cells. Interestingly, we found that TNF signaling and gene expression were significantly attenuated in RNF186-KO Ls174t cells compared with wild-type control cells (Fig. 2A, 2B). Consistently, overexpression of RNF186 in Ls174t cells caused significant upregulation of multiple proinflammatory genes, such as TNF, CXCL1, and IL-6, among others, and many

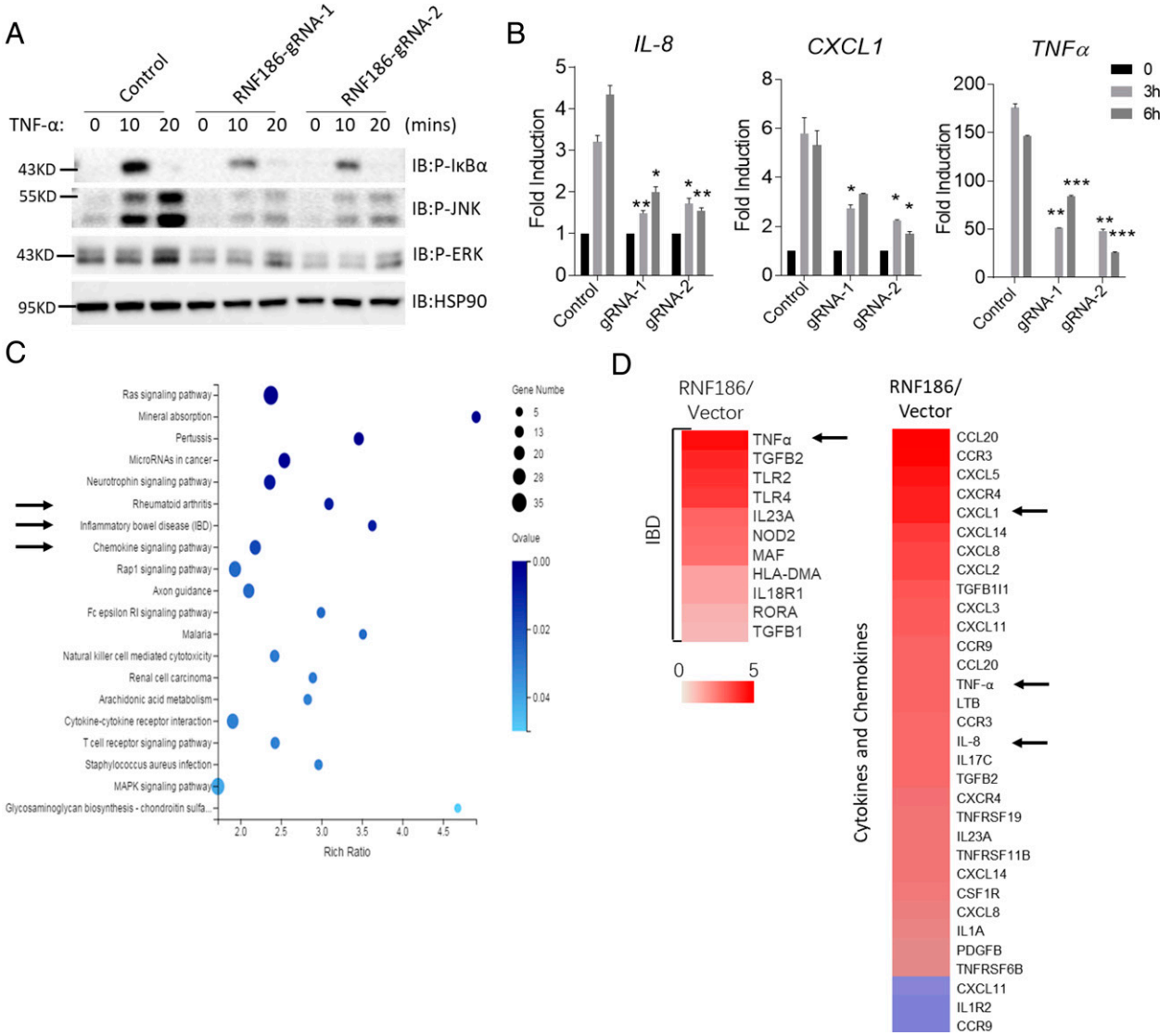

FIGURE 2. RNF186 is required for TNF-induced signaling activation in colorectal epithelial cells. (**A** and **B**) Control Ls174t cells or RNF186-KO Ls174t cells were treated with TNF (100 ng/ml) for the indicated time, followed by Western blot or RT and real-time PCR analysis of indicated proteins (A) or mRNA (B) expression. (**C**) The whole transcriptome from control Ls174t cells or RNF186-overexpressed Ls174t cells is shown by cluster analysis. (**D**) Heatmaps of RNA-seq data are shown. $*p < 0.05$, $**p < 0.01$, $***p < 0.001$ based on two-sided unpaired *t* test for (B). All error bars represent SEM of technical replicates. Data are representative of three independent experiments except for (C) and (D). IBD, inflammatory bowel disease.

of the upregulated genes clustered in autoimmune diseases, such as inflammatory bowel disease and rheumatoid arthritis (Fig. 2C, 2D). We did not find any expressional difference of cytokines between EPHB2−wild-type cells and EPHB2-KO cells after LPS or poly(I:C) stimulations (Supplemental Fig. 1C, 1D). Taken together, these data indicate that RNF186 is critical for the activation of the TNF signaling pathway in colorectal epithelial cells.

Ubiquitination of EPHB2 is critical for TNF signaling activation in colorectal epithelial cells

In a previous study, we found that RNF186 cataloged EPHB2 ubiquitination at the K788 and K892 sites, and ubiquitination of the K892 site in EPHB2 played an essential role in ephrin-B1−induced autophagy in colorectal epithelial cells (28). Surprisingly, overexpression of both EPHB2 K892R and K788R mutants yielded defective TNF-induced signaling activation and proinflammatory gene expression compared with wild-type EPHB2 in Ls174t cells (Supplemental Fig. 2A, 2B). Consistently, NF-κB activation was also significantly reduced when EPHB2 K788R or K892R was overexpressed compared with wild-type EPHB2 (Supplemental Fig. 2C). Taken together, these data suggest that both K788 and K892 of EPHB2 were ubiquitinated after TNF stimulation, and ubiquitination of both sites of K788 and K892 may contribute to TNF-induced signal transduction. Next, we mutated both lysine residues 788 and 892 of EPHB2 to arginine and examined the impact of the double EPHB2 KR mutation on the TNF signaling pathway. TNF promoted ubiquitination of wild-type EPHB2 but not the EPHB2 KR mutant after TNF stimulation (Fig. 3A). We examined the ubiquitination type of EPHB2 mediated by RNF186 and found that the ubiquitination of EPHB2 is predominantly mediated by K63 and K27 conjugation, but not by K48 conjugation (Supplemental Fig. 3A−C). Overexpression of the EPHB2 KR mutant significantly reduced signaling activation and proinflammatory gene expression

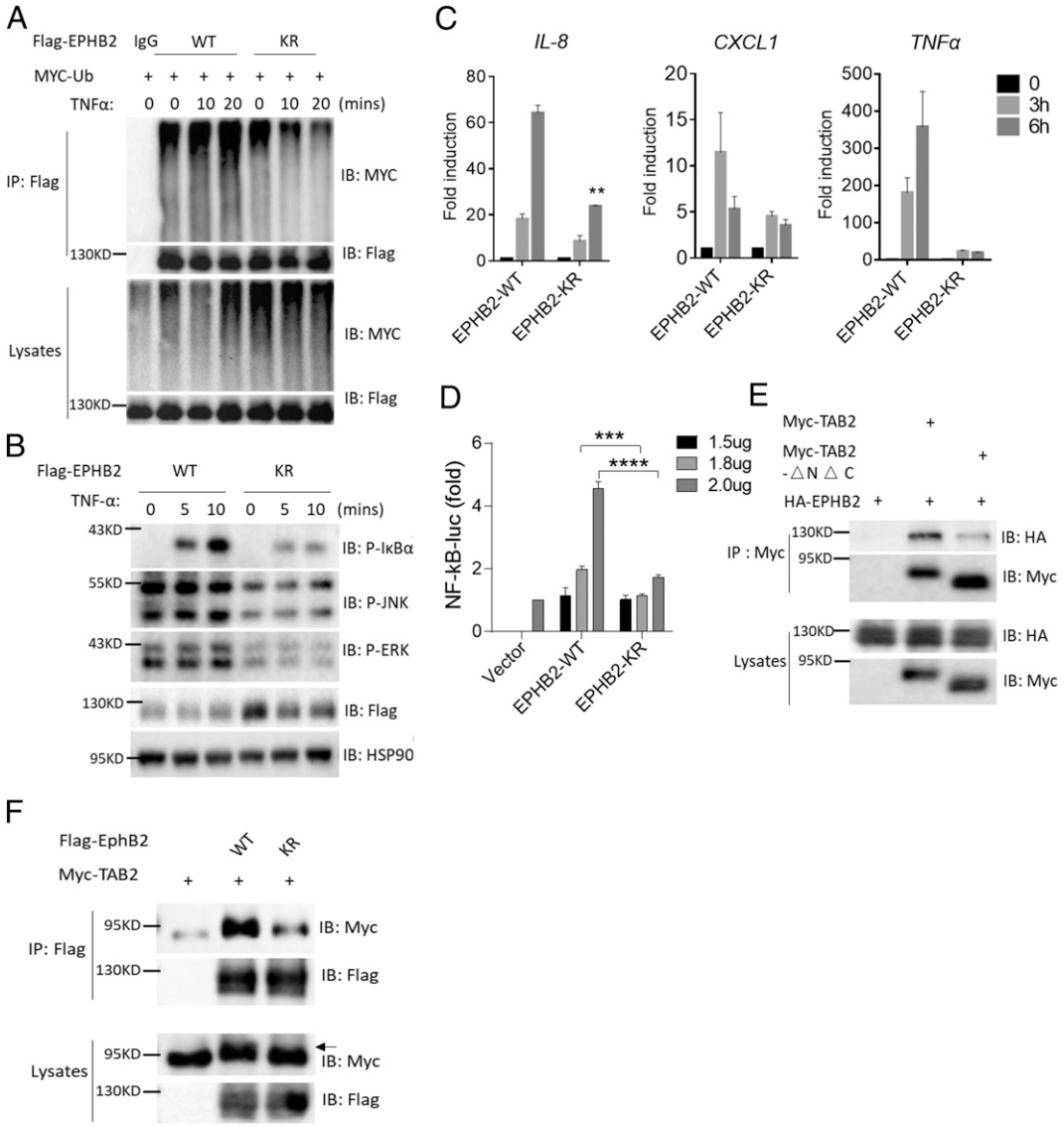

FIGURE 3. Ubiquitination of EPHB2 is required for TNF-induced signaling activation in colorectal epithelial cells. (**A**) 293T cells were transfected as indicated, and cell lysates were immunoprecipitated by anti-FLAG Ab according to the in vivo ubiquitination experiment described in *Materials and Methods*, followed by Western blot analysis of the indicated proteins. (**B** and **C**) EPHB2-KO 293T cells were transfected with indicated plasmids for 24 h, and cells were stimulated with TNF (50 ng/ml) for the indicated time, followed by Western blot (B) or RT and real-time PCR (C) analysis of indicated proteins. (**D**) 293T cells were transfected with indicated plasmids for 24 h, followed by reporter assay analysis of NF-κB activity. (**E** and **F**) 293T cells were transfected as indicated, and cell lysates were immunoprecipitated by anti-Myc Ab (E) or anti-FLAG Ab (F), followed by Western blot analysis of the indicated proteins. The arrow in (F) indicates slower migration of the TAB2 band. $^{**}p < 0.01$, $^{***}p < 0.001$, $^{****}p < 0.0001$ based on two-sided unpaired *t* test for (C) and (D). All error bars represent SEM of technical replicates. Data are representative of three independent experiments.

compared with overexpression of wild-type EPHB2 after TNF stimulation (Fig. 3B, 3C). Consistently, overexpression of the EPHB2 KR mutant significantly reduced NF-κB activation compared with wild-type EPHB2 (Fig. 3D). Taken together, these data indicate that ubiquitination of EPHB2 at K788 and K892 is critical for TNF-induced signal transduction. It was reported that TAB2 and TAB3 could bind the ubiquitin chain through their CUE and NZF domains and mediate signal transduction in the TNF signaling pathway (30, 31). We found that EPHB2 interacted with TAB2, and deletion of the CUE and NZF domains of TAB2 decreased the interaction with EPHB2 (Fig. 3E). We further found that the KR mutant of EPHB2 showed a significantly reduced interaction with TAB2, suggesting that the interaction between EPHB2 and TAB2 occurs mostly through ubiquitination of EPHB2 (Fig. 3F). Taken together, these data indicate that ubiquitination of EPHB2 is essential for TNF-induced signal transduction, and, most likely, ubiquitinated EPHB2 recruits TAB2 for downstream signal transduction.

Phosphorylation of TAB2 by EPHB2 is essential for TNF signaling activation

EPHB2 is a tyrosine kinase receptor, and we explored whether the kinase activity of EPHB2 played any role in TNF-induced signal transduction. We found that overexpression of an EPHB2 kinase-dead (KD) mutant or EPHB2 phosphorylation site mutant significantly reduced TNF-induced signaling activation and proinflammatory gene expression (Fig. 4A, 4B). We found that coexpression of wild-type EPHB2 but not the KD mutant of EPHB2 with TAB2 caused slower migration of TAB2 on the SDS gel. These results suggest that TAB2 may be phosphorylated by EPHB2 (Fig. 3F). We found that wild-type EPHB2, but not the EPHB2 KD mutant, could phosphorylate TAB2 based on a kinase assay (Fig. 4C). To further understand the phosphorylation sites of TAB2 by EPHB2, we co-overexpressed EPHB2 and TAB2 and identified phosphorylation sites of TAB2 by mass spectrometry. Five tyrosine sites of TAB2, that is, Y88, Y368, Y388, Y532, and Y632, were identified as phosphorylation sites by EPHB2 (Fig. 4D). We mutated all five tyrosine residues to phenylalanine (TAB2 Y5F) and examined whether TAB2 Y5F completely lost its phosphorylation. Surprisingly, TAB2 Y5F still showed residual phosphorylation by EPHB2. These data indicate that in addition to these five tyrosine sites, TAB2 can be phosphorylated by EPHB2 at other sites (Supplemental Fig. 3D). In addition to the five tyrosine sites that are phosphorylated by EPHB2 identified by mass spectrometry, there were five tyrosine sites of Y53, Y55, Y214, Y218, and Y462 that were not phosphorylated by EPHB2 identified by mass spectrometry. Therefore, four other tyrosine sites, that is, Y248, Y284, Y312, and Y497, of TAB2 may be phosphorylated by EPHB2. Then, we further generated a Y9F mutant of TAB2, which included an additional four tyrosines of Y248, Y284, Y312, and Y497 in addition to Y5F. We found that Y9F

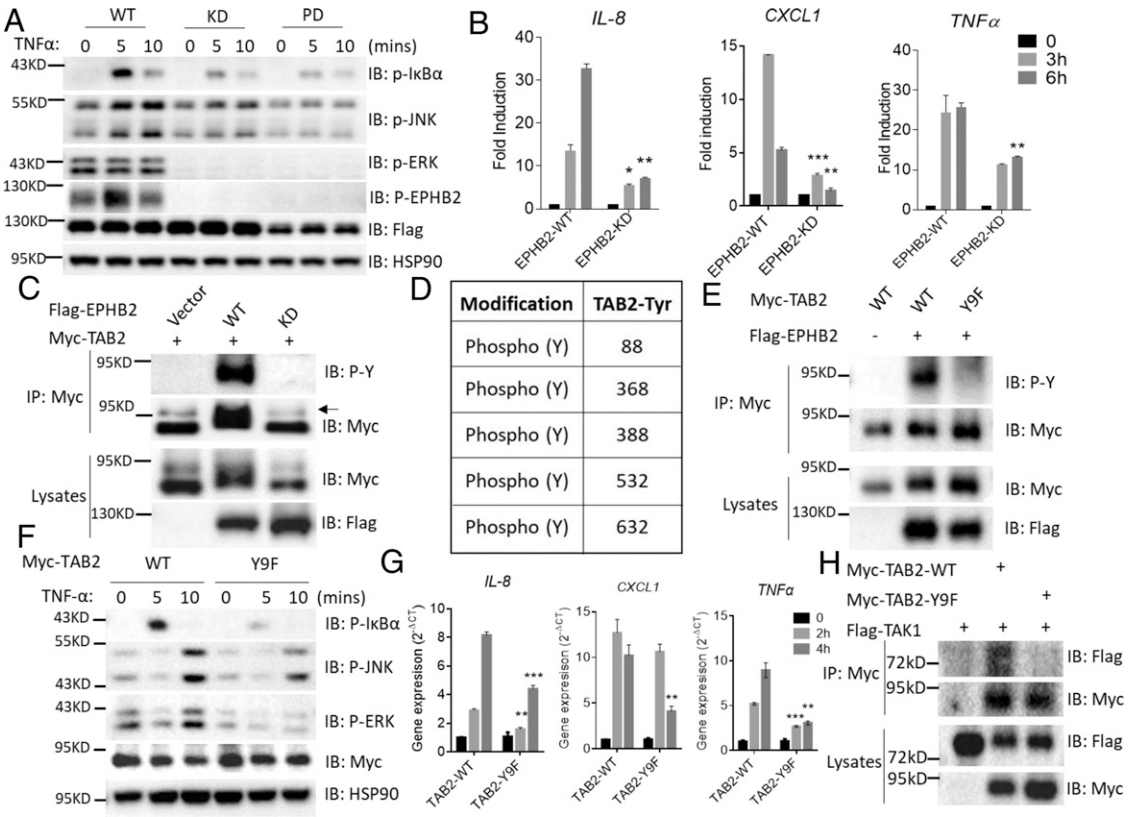

FIGURE 4. TAB2 is phosphorylated by EPHB2 after TNF stimulation. (**A** and **B**) EPHB2-KO 293T cells were transfected with indicated plasmids for 24 h, and cells were stimulated with TNF (50 ng/ml) for the indicated time, followed by Western blot (A) or RT and real-time PCR (B) analysis of indicated proteins. (**C**) 293T cells were transfected as indicated, and cell lysates were immunoprecipitated by anti-Myc Ab, followed by Western blot analysis of the indicated proteins. Arrow indicates slower migration of the TAB2 band. (**D**) The phosphorylation sites of TAB2 by EPHB2 identified by mass spectrometry are shown. (**E**) EPHB2-KO 293T cells were transfected with indicated plasmids for 24 h, and cell lysates were immunoprecipitated by anti-Myc Ab, followed by Western blot analysis of the indicated proteins. (**F** and **G**) EPHB2-KO 293T cells were transfected with indicated plasmids for 24 h, and cells were stimulated with TNF (50 ng/ml) for the indicated time, followed by Western blot (F) or RT and real-time PCR analysis (G) of indicated proteins. (**H**) 293T cells were transfected as indicated, and cell lysates were immunoprecipitated by anti-Myc Ab, followed by Western blot analysis of the indicated proteins. $*p < 0.05$, $**p < 0.01$, $***p < 0.001$ based on two-sided unpaired t test for (B) and (G). All error bars represent SEM of technical replicates. Data are representative of three independent experiments.

of TAB2 completely lost phosphorylation when coexpressed with EPHB2, and overexpression of TAB2 Y9F significantly reduced TNF-induced signaling activation and proinflammatory gene expression (Fig. 4E–G). Taken together, these data indicate that phosphorylation of TAB2 at nine tyrosine sites by EPHB2 is critical for TNF-induced signal transduction. The functional role of TAB2 in the TNF signaling pathway is to recruit kinase TAK1 for downstream IKK complex activation, and we found that Y9F of TAB2 completely lost its interaction with TAK1 (Fig. 4H). These data indicate that the phosphorylation of TAB2 by EPHB2 is essential for its binding to TAK1.

RNF186-KO mice showed attenuated colorectal tumorigenesis

The TNF signaling pathway is critical for colorectal carcinogenesis, especially for chronic inflammation-induced tumor formation in the colon (26). Next, we examined the phenotype of RNF186-KO mice in DSS+AOM-induced colitis-propelled colorectal tumorigenesis. Consistent with our previous study, after DSS+AOM treatment, RNF186-KO mice showed significantly faster weight loss compared with control mice, and these data indicate that RNF186 plays a protective role in DSS-induced colorectal inflammation (Fig. 5A). Interestingly, although RNF186-KO mice had faster weight loss compared control mice, the colorectal tumor number and size were significantly reduced compared with those of control mice (Fig. 5B, 5C). Consistent with the in vitro data, NF-κB and JNK activation in the tumors of RNF186 KO mice was significantly reduced compared with that in the tumors of control mice. In contrast, p-ERK and p-STAT3 showed a trend of reduction in the tumors of RNF186-KO mice, but the difference did not reach significance (Fig. 5D). Consistent with the in vitro study, the gene expression of *TNF* was significantly reduced in the tumors from RNF186-KO mice compared with control mice. In contrast, the other proinflammatory genes, such as *CXCL1*, *IL-1β*, and *IL-6*, showed a trend of reduction, whereas the difference did not reach significance (Fig. 5E). Interestingly, the expression of genes related to cell proliferation, such as cyclin D1, cyclin D2, and cyclin D3, was significantly reduced in the tumors from RNF186-KO mice compared with those from control mice (Fig. 5E). Taken together, these data indicate that RNF186-mediated TNF signaling activation plays a critical role in colitis-propelled colorectal tumorigenesis.

To further confirm that the reduced colorectal tumorigenesis phenotype observed in RNF186-KO mice is due to defective TNF signaling activation, we examined DSS+AOM-induced colitis-propelled colorectal tumorigenesis after treatment of control mice and RNF186-KO mice with the TNF antagonist R7050. Interestingly, after blockade of TNF signaling with R7050, RNF186-KO mice still showed faster weight loss compared with control mice in the DSS+AOM model, and these data suggest that defective TNF signaling in the colorectal epithelial cells of RNF186-KO mice does not account for the more severe phenotype of colorectal inflammation (Supplemental Fig. 4A). Tumor size and tumor number were similar between control mice and RNF186-KO mice after R7050 treatment in the DSS+AOM-induced tumorigenesis model, and the gene expression from tumors of control mice and RNF186-KO mice was also comparable (Supplemental Fig. 4B–D). Taken together, these data further confirmed that defective TNF signaling activation in the colorectal epithelial cells of RNF186-KO mice accounts for the attenuated phenotype of colitis-propelled colorectal tumorigenesis.

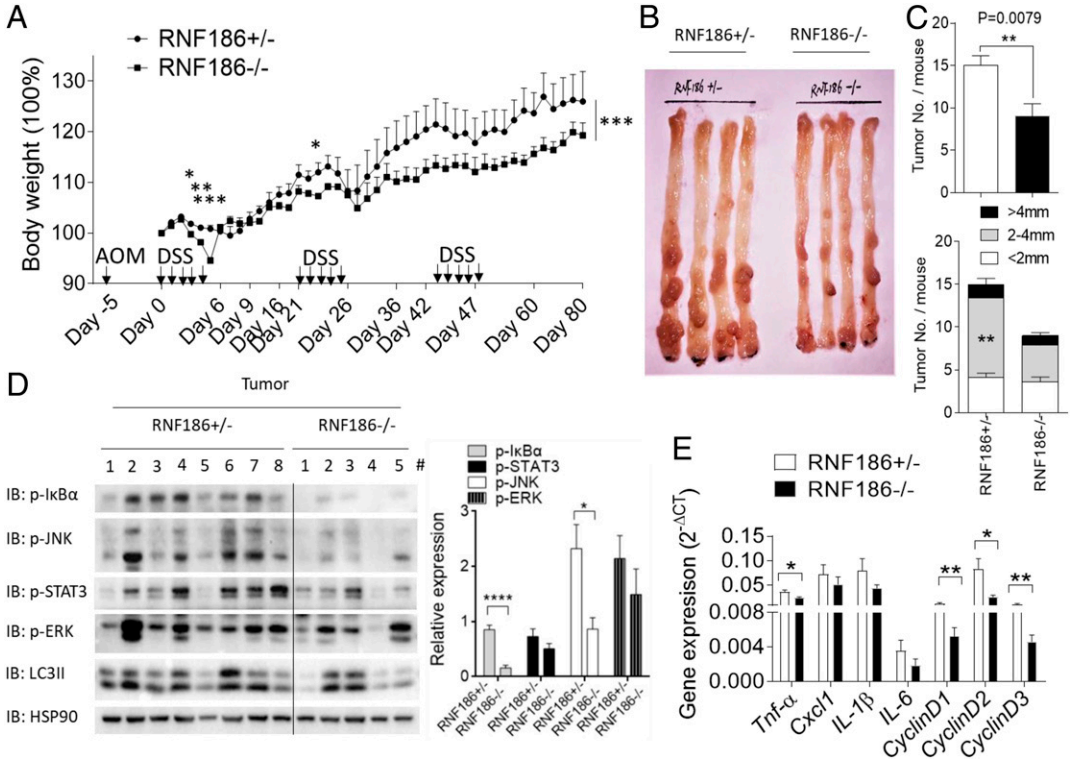

FIGURE 5. RNF186-KO mice showed attenuated colorectal tumorigenesis. (**A**) Weight changes of control mice and RNF186-KO mice in the process of DSS+AOM-induced tumorigenesis is shown. (**B** and **C**) Image of colonic tumor from control mice and RNF186-KO mice is shown (B) The colonic tumor number from control mice and RNF186-KO mice is shown (C). (**D**) The lysates of colonic tumors from control mice and RNF186-KO mice were analyzed by Western blot. Quantitative data are shown in the right panel. (**E**) The lysates of colonic tumors from control mice and RNF186-KO mice were analyzed by RT and real-time PCR. $*p < 0.05$, $**p < 0.01$, $***p < 0.001$, $****p < 0.0001$ based on two-sided unpaired t test for (A) and (C)–(E) and two-way ANOVA for (A). All error bars represent SEM of technical replicates. Data are representative of three independent experiments.

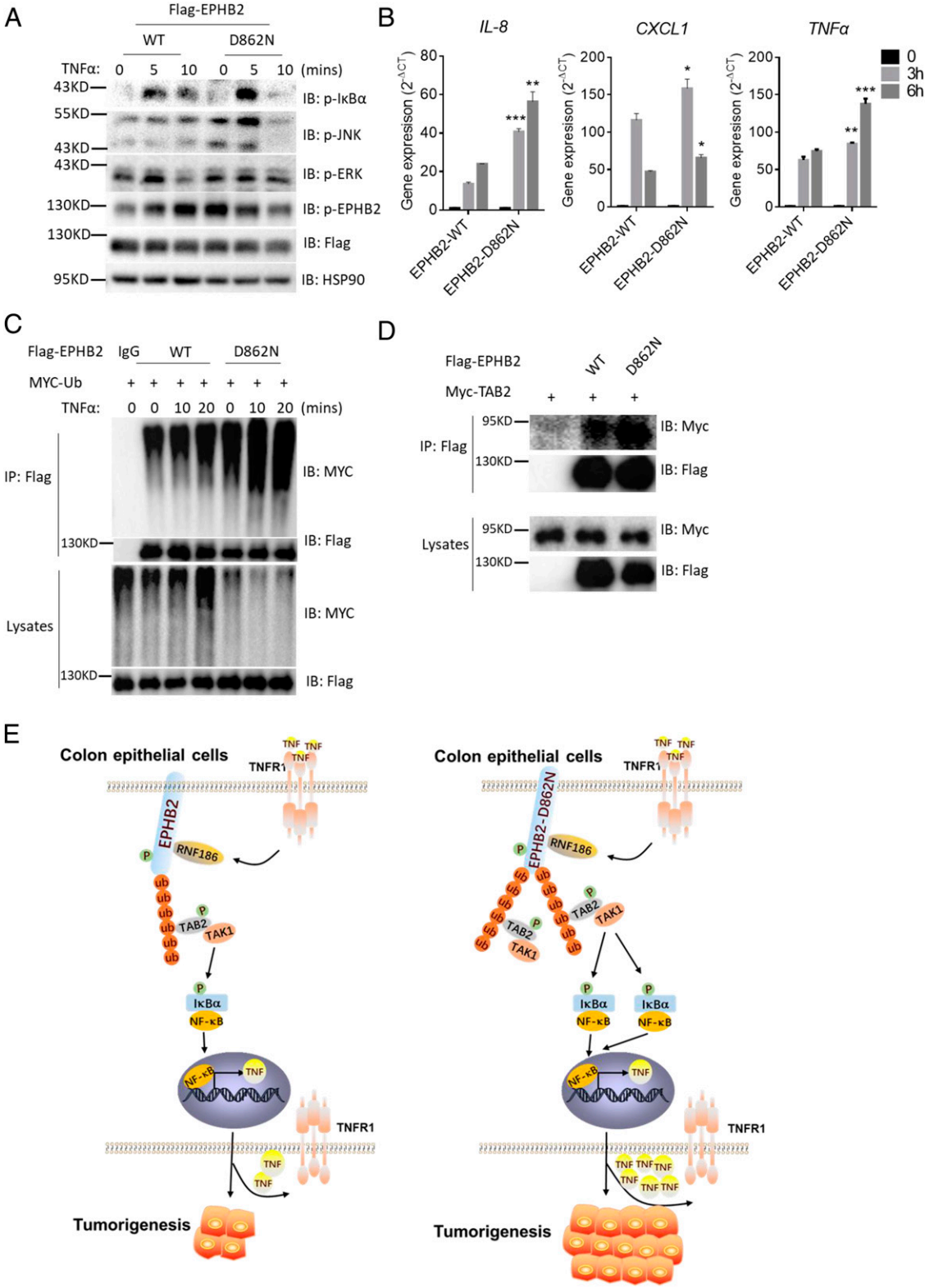

FIGURE 6. EPHB2 D862N is a gain-of-function mutant. (**A** and **B**) 293T cells were transfected with indicated plasmids for 24 h, and cells were stimulated with TNF (50 ng/ml) for the indicated time, followed by Western blot (A) or RT and real-time PCR (B) analysis of indicated proteins. (**C**) 293T cells were transfected with the plasmids as indicated, and cell lysates were immunoprecipitated by anti-FLAG Ab according to the in vivo ubiquitination experiment described in *Materials and Methods*, followed by Western blot analysis of the indicated proteins. (**D**) 293T cells were transfected the plasmids as indicated, and cell lysates were immunoprecipitated by anti-FLAG Ab, followed by Western blot analysis of the indicated proteins. (**E**) Overall model of functional role of the RNF186/EPHB2 axis in the TNF signaling pathway is shown. After TNF stimulation, EPHB2 is ubiquitinated by RNF186, followed by recruiting and phosphorylating TAB2 for the binding and activating of TAK1, which activates the NF-κB signaling pathway for the production of tumor-promoting cytokines, such as TNF. EPHB2-D862N is a gain-of-function mutant, which has increased affinity to TAB2 due to increased ubiquitination by RNF186. EPHB2-D862N more strongly activates the NF-κB signaling pathway and leads to increased TNF production for the tumorigenesis. $*p < 0.05$, $**p < 0.01$, $***p < 0.001$ based on two-sided unpaired *t* test for (B). All error bars represent SEM of technical replicates. Data are representative of three independent experiments.

EPHB2 D862N is a gain-of-function mutant

One study identified an EPHB2 genetic mutation, D862N, in a family of colorectal cancer, and we explored the function of this mutation in the TNF signaling pathway. Interestingly, overexpression of EPHB2 D862N led to increased EPHB2 phosphorylation compared with wild-type EPHB2 at the basal condition, and signaling activation was significantly increased after EPBH2 D862N overexpression (Fig. 6A). Consistent with the signaling activation, proinflammatory gene expression was significantly increased in the cells overexpressing EPHB2 D862N compared with wild-type control cells (Fig. 6B). Next, we examined the ubiquitination condition of EPHB2 D862N in the TNF signaling pathway. Interestingly, the ubiquitination of EPHB2 D862N was significantly increased compared with wild-type EPHB2 after TNF stimulation (Fig. 6C). We further found that the EPHB2 D862N mutant showed a significantly increased interaction with TAB2 compared with wild-type EPHB2 (Fig. 6D). Overall, these data indicate that EPHB2 D862N is a gain-of-function mutant and that EPHB2 kinase activity may promote colorectal tumorigenesis.

Discussion

In the current study, we reported a novel EPHB2-RNF186-TAB2–mediated TNF signaling cascade in colonic epithelial cells, and this pathway is essential for colonic tumorigenesis. We found that after TNF stimulation, EPHB2 was ubiquitinated by RNF186, followed by recruiting and phosphorylating TAB2 for the binding and activating of TAK1, which activates NF-κB signaling pathway for the production of tumor-promoting cytokines, such as TNF. Interestingly, we found that EPHB2-D862N, a genetic mutant of EPHB2 identified in colorectal cancer patients, is a gain-of-function mutant, which has increased affinity to TAB2 due to increased ubiquitination by RNF186. EPHB2-D862N more strongly activates the NF-κB signaling pathway compared with wild-type EPHB2, and this leads to increased TNF production for the tumorigenesis (Fig. 6E). Overall, this study not only identifies a novel mechanism for TNF signal transduction in colonic epithelial cells but also provides potential targets for the treatment of human colorectal cancer.

EPHB2 molecules are related to the tumorigenesis of many cancer types, especially colorectal cancer. However, the role of EPHB2 in human cancer is controversial. Some of the studies suggest that EPHB2 is a tumor suppressor. For example, one study found that most human colorectal cancers lose EPHB2 expression, which was strongly correlated with the degree of malignancy of the cancer (4). Another study found that EPHB2-mediated compartmentalization helped to restrict the spreading of colorectal cancer cells (10). Another study found that the tyrosine kinase activity of EPHB2 regulated colorectal cancer cell proliferation through the Abl–cyclin D1 pathway (11). A retrospective study found that higher EPHB2 expression levels in human colorectal cancer were associated with a better prognosis than lower EPHB2 expression levels (14). Some other studies showed that EPHB2 could also function as an oncogene, and EPHB2 expression levels in cancer tissues predict patient prognosis. For example, one study found that a mAb targeting EPHB2 showed a therapeutic effect on mouse colorectal cancer (16). Other studies found that several *EPHB2* gene mutations were identified in colorectal cancer (13). The discrepancy in the role of EPHB2 in cancer may be due to the different cancer models employed, or EPHB2 may have different functional roles in different cancer types. Another possibility is that EPHB2 is widely expressed in different cell types, and EPHB2 expression in different cell types may contribute differently to certain cancers. Our study showed that EPHB2 is essential for TNF signal transduction in colonic epithelial cells and mediates colorectal tumorigenesis in a chronic inflammation-induced colon cancer model. Therefore, EPHB2 may represent a potential target for the treatment of colorectal cancer, as suggested by a similar study (16). EPHB2 is a tyrosine kinase, and we found that its tyrosine kinase activity was involved in the activation of TNF signal transduction in colonic epithelial cells (Fig. 4). Therefore, small molecular compounds targeting the kinase activity of EPHB2 may represent a good therapeutic option for the treatment of colorectal cancer. In our previous study, we showed that two broad-spectrum tyrosine kinase inhibitors, dasatinib and vandetanib, strongly inhibit EPHB2 kinase activity and exhibit a therapeutic effect on EAE (32). Future studies need to explore more specific small molecular inhibitors of EPHB2, and the inhibition of EPHB2 kinase activity may have multiple uses in different diseases.

Disclosures

S.L. is employed by Wuhan Biobank Co., Ltd. The other authors have no financial conflicts of interest.

References

1. Barquilla, A., and E. B. Pasquale. 2015. Eph receptors and ephrins: therapeutic opportunities. *Annu. Rev. Pharmacol. Toxicol.* 55: 465–487.
2. Pasquale, E. B. 2008. Eph-ephrin bidirectional signaling in physiology and disease. *Cell* 133: 38–52.
3. Adams, R. H., G. A. Wilkinson, C. Weiss, F. Diella, N. W. Gale, U. Deutsch, W. Risau, and R. Klein. 1999. Roles of ephrinB ligands and EphB receptors in cardiovascular development: demarcation of arterial/venous domains, vascular morphogenesis, and sprouting angiogenesis. *Genes Dev.* 13: 295–306.
4. Batlle, E., J. Bacani, H. Begthel, S. Jonkheer, A. Gregorieff, M. van de Born, N. Malats, E. Sancho, E. Boon, T. Pawson, et al. 2005. EphB receptor activity suppresses colorectal cancer progression. [Published erratum appears in 2005 *Nature* 436: 881.] *Nature* 435: 1126–1130.
5. Batlle, E., J. T. Henderson, H. Beghtel, M. M. van den Born, E. Sancho, G. Huls, J. Meeldijk, J. Robertson, M. van de Wetering, T. Pawson, and H. Clevers. 2002. β-Catenin and TCF mediate cell positioning in the intestinal epithelium by controlling the expression of EphB/ephrinB. *Cell* 111: 251–263.
6. Dalva, M. B., M. A. Takasu, M. Z. Lin, S. M. Shamah, L. Hu, N. W. Gale, and M. E. Greenberg. 2000. EphB receptors interact with NMDA receptors and regulate excitatory synapse formation. *Cell* 103: 945–956.
7. Henkemeyer, M., O. S. Itkis, M. Ngo, P. W. Hickmott, and I. M. Ethell. 2003. Multiple EphB receptor tyrosine kinases shape dendritic spines in the hippocampus. *J. Cell Biol.* 163: 1313–1326.
8. Holmberg, J., M. Genander, M. M. Halford, C. Annerén, M. Sondell, M. J. Chumley, R. E. Silvany, M. Henkemeyer, and J. Frisén. 2006. EphB receptors coordinate migration and proliferation in the intestinal stem cell niche. *Cell* 125: 1151–1163.
9. Pasquale, E. B. 2010. Eph receptors and ephrins in cancer: bidirectional signalling and beyond. *Nat. Rev. Cancer* 10: 165–180.
10. Cortina, C., S. Palomo-Ponce, M. Iglesias, J. L. Fernández-Masip, A. Vivancos, G. Whissell, M. Humà, N. Peiró, L. Gallego, S. Jonkheer, et al. 2007. EphB-ephrin-B interactions suppress colorectal cancer progression by compartmentalizing tumor cells. *Nat. Genet.* 39: 1376–1383.
11. Genander, M., M. M. Halford, N. J. Xu, M. Eriksson, Z. Yu, Z. Qiu, A. Martling, G. Greicius, S. Thakar, T. Catchpole, et al. 2009. Dissociation of EphB2 signaling pathways mediating progenitor cell proliferation and tumor suppression. *Cell* 139: 679–692.
12. Merlos-Suárez, A., F. M. Barriga, P. Jung, M. Iglesias, M. V. Céspedes, D. Rossell, M. Sevillano, X. Hernando-Momblona, V. da Silva-Diz, P. Muñoz, et al. 2011. The intestinal stem cell signature identifies colorectal cancer stem cells and predicts disease relapse. *Cell Stem Cell* 8: 511–524.
13. Alazzouzi, H., V. Davalos, A. Kokko, E. Domingo, S. M. Woerner, A. J. Wilson, L. Konrad, P. Laiho, E. Espín, M. Armengol, et al. 2005. Mechanisms of inactivation of the receptor tyrosine kinase EPHB2 in colorectal tumors. *Cancer Res.* 65: 10170–10173.
14. Lugli, A., H. Spichtin, R. Maurer, M. Mirlacher, J. Kiefer, P. Huusko, D. Azorsa, L. Terracciano, G. Sauter, O. P. Kallioniemi, et al. 2005. EphB2 expression across 138 human tumor types in a tissue microarray: high levels of expression in gastrointestinal cancers. *Clin. Cancer Res.* 11: 6450–6458.
15. Huusko, P., D. Ponciano-Jackson, M. Wolf, J. A. Kiefer, D. O. Azorsa, S. Tuzmen, D. Weaver, C. Robbins, T. Moses, M. Allinen, et al. 2004. Nonsense-mediated decay microarray analysis identifies mutations of EPHB2 in human prostate cancer. *Nat. Genet.* 36: 979–983.
16. Mao, W., E. Luis, S. Ross, J. Silva, C. Tan, C. Crowley, C. Chui, G. Franz, P. Senter, H. Koeppen, and P. Polakis. 2004. EphB2 as a therapeutic antibody drug target for the treatment of colorectal cancer. *Cancer Res.* 64: 781–788.
17. Chen, G., and D. V. Goeddel. 2002. TNF-R1 signaling: a beautiful pathway. *Science* 296: 1634–1635.
18. Baud, V., and M. Karin. 2001. Signal transduction by tumor necrosis factor and its relatives. *Trends Cell Biol.* 11: 372–377.
19. Blonska, M., P. B. Shambharkar, M. Kobayashi, D. Zhang, H. Sakurai, B. Su, and X. Lin. 2005. TAK1 is recruited to the tumor necrosis factor-α (TNF-α)

receptor 1 complex in a receptor-interacting protein (RIP)-dependent manner and cooperates with MEKK3 leading to NF-κB activation. *J. Biol. Chem.* 280: 43056–43063.
20. Jackson-Bernitsas, D. G., H. Ichikawa, Y. Takada, J. N. Myers, X. L. Lin, B. G. Darnay, M. M. Chaturvedi, and B. B. Aggarwal. 2007. Evidence that TNF-TNFR1-TRADD-TRAF2-RIP-TAK1-IKK pathway mediates constitutive NF-κB activation and proliferation in human head and neck squamous cell carcinoma. *Oncogene* 26: 1385–1397.
21. Terzić, J., S. Grivennikov, E. Karin, and M. Karin. 2010. Inflammation and colon cancer. *Gastroenterology* 138: 2101–2114.e5.
22. Sethi, G., B. Sung, and B. B. Aggarwal. 2008. TNF: a master switch for inflammation to cancer. *Front. Biosci.* 13: 5094–5107.
23. Zhu, M., Y. Zhu, and P. Lance. 2013. TNFα-activated stromal COX-2 signalling promotes proliferative and invasive potential of colon cancer epithelial cells. *Cell Prolif.* 46: 374–381.
24. Hyun, Y. S., D. S. Han, A. R. Lee, C. S. Eun, J. Youn, and H. Y. Kim. 2012. Role of IL-17A in the development of colitis-associated cancer. *Carcinogenesis* 33: 931–936.
25. De Simone, V., E. Franzè, G. Ronchetti, A. Colantoni, M. C. Fantini, D. Di Fusco, G. S. Sica, P. Sileri, T. T. MacDonald, F. Pallone, et al. 2015. Th17-type cytokines, IL-6 and TNF-α synergistically activate STAT3 and NF-kB to promote colorectal cancer cell growth. *Oncogene* 34: 3493–3503.
26. Popivanova, B. K., K. Kitamura, Y. Wu, T. Kondo, T. Kagaya, S. Kaneko, M. Oshima, C. Fujii, and N. Mukaida. 2008. Blocking TNF-α in mice reduces colorectal carcinogenesis associated with chronic colitis. *J. Clin. Invest.* 118: 560–570.
27. Nikiteas, N. I., N. Tzanakis, M. Gazouli, G. Rallis, K. Daniilidis, G. Theodoropoulos, A. Kostakis, and G. Peros. 2005. Serum IL-6, TNFα and CRP levels in Greek colorectal cancer patients: prognostic implications. *World J. Gastroenterol.* 11: 1639–1643.
28. Zhang, H., Z. Cui, D. Cheng, Y. Du, X. Guo, R. Gao, J. Chen, W. Sun, R. He, X. Ma, et al. 2021. RNF186 regulates EFNB1 (ephrin B1)-EPHB2-induced autophagy in the colonic epithelial cells for the maintenance of intestinal homeostasis. *Autophagy* 17: 3030–3047.
29. Beaudoin, M., P. Goyette, G. Boucher, K. S. Lo, M. A. Rivas, C. Stevens, A. Alikashani, M. Ladouceur, D. Ellinghaus, L. Törkvist, et al.; International IBD Genetics Consortium. 2013. Deep resequencing of GWAS loci identifies rare variants in *CARD9*, *IL23R* and *RNF186* that are associated with ulcerative colitis. *PLoS Genet.* 9: e1003723.
30. Kanayama, A., R. B. Seth, L. Sun, C. K. Ea, M. Hong, A. Shaito, Y. H. Chiu, L. Deng, and Z. J. Chen. 2004. TAB2 and TAB3 activate the NF-κB pathway through binding to polyubiquitin chains. *Mol. Cell* 15: 535–548.
31. Tian, Y., Y. Zhang, B. Zhong, Y. Y. Wang, F. C. Diao, R. P. Wang, M. Zhang, D. Y. Chen, Z. H. Zhai, and H. B. Shu. 2007. RBCK1 negatively regulates tumor necrosis factor- and interleukin-1-triggered NF-κB activation by targeting TAB2/3 for degradation. *J. Biol. Chem.* 282: 16776–16782.
32. Chen, J., R. He, W. Sun, R. Gao, Q. Peng, L. Zhu, Y. Du, X. Ma, X. Guo, H. Zhang, et al. 2020. TAGAP instructs Th17 differentiation by bridging Dectin activation to EPHB2 signaling in innate antifungal response. *Nat. Commun.* 11: 1913.